



Toward an International StormWatch Using Wide Swath SAR

Robert C. Beal

Wide swath synthetic aperture radar (SAR), exemplified by the multibeam ScanSAR modes of Radarsat, can potentially deliver global near-real-time coastal wind fields with nearly 2 orders of magnitude greater spatial resolution (≈ 300 m) than conventional (active or passive) scatterometers (≈ 25 km). But this superior resolution comes with caveats. An understanding of the small-scale ocean scattering physics, necessary to fully describe the complex relationship between wind and radar backscatter, remains incomplete. End-to-end calibration of multibeam SARs is difficult and still largely undemonstrated. And methods for nesting the intrinsically high-resolution SAR wind estimates within those of the coarser numerical models, scatterometers, radiometers, and surface buoys are still in their infancy. Despite these caveats, ScanSAR offers a unique new tool for probing the wind field over the ocean. To illustrate, one especially compelling example from a Radarsat ScanSAR pass over the U.S. East Coast is described. (Keywords: Radarsat, SAR wind fields, ScanSAR, synthetic aperture radar.)

INTRODUCTION

The synthesis of long apertures to obtain very high resolution from aircraft using radar technology was first demonstrated by Carl Wiley at Goodyear Aerospace in 1951.¹ Early synthetic aperture radars (SARs) lacked the advantage of today's rapid computer processing and large digital memories for signal correlation. These SARs initially relied on electronic delay lines and later on coherent optical processing.² Although early processing was slow and cumbersome, the fundamental principles of radar aperture synthesis were well established by the early 1960s. High-resolution aircraft SAR

systems provided all-weather, 24-h military reconnaissance. Raney³ provides a comprehensive review of both the history and technology of SAR.

In the early 1970s, the U.S. National Aeronautics and Space Administration (NASA) Jet Propulsion Laboratory proposed a spacecraft SAR to map the perpetually cloud-covered surface of Venus. The Venus Orbiter Imaging Radar (VOIR), as it was initially named, languished unrealized until it became the (more sophisticated) Magellan Venus Mapping Mission of the 1990s. Meanwhile, the original VOIR design evolved

into the 1978 Earth-oriented L-band Seasat SAR,⁴ which sent back hundreds of provocative ocean images during its abbreviated 98-day lifetime. Nothing comparable was launched—except for the short-term Shuttle Imaging Radar (SIR) series, most notably the NASA/German/Italian SIR-C/X SAR⁵—until the European Space Agency’s well-calibrated C-band European Remote Sensing satellite (ERS-1) SAR in 1991.⁶ Since 1991, the scientific community has always had access to at least one SAR, with data routinely available to approved investigators. The ERS-1 SAR was followed by the L-band Japanese Earth Resources Satellite (JERS-1) SAR in 1992, another C-band ERS-2 SAR in April 1995, and finally the Canadian C-band Radarsat⁷ in November 1995.

Until Radarsat, the maximum swath width of any previously orbiting SAR had been 100 km, a parameter tightly constrained by the need to (1) “fill the aperture” and (2) receive all the returned energy between transmitter pulses. To bypass these constraints, Radarsat employed the ScanSAR^{8,9} technique. Through the use of multiple electronically steered antenna beams and carefully synchronized transmitter pulse timing, Radarsat can achieve 525-km swaths (at an altitude of 800 km) using four beams. Even wider swaths may be possible using up to eight beams (see the article by Holt and Hilland, this issue). Calibration is more difficult for these wide multibeam swaths, however, than for a single beam. Even 4 years after the launch of Radarsat (80% of its planned 5-year lifetime), some of its ScanSAR modes still lacked adequate calibration and stability for satisfactory backscatter-to-wind-speed inversion (see, e.g., articles in this issue by Vachon et al., Gower and Skey, and Horstmann et al.). But inversion is only partially an engineering problem. Although radar backscatter increases monotonically with wind speed (all other parameters being constant), the rate of increase is very low for high winds and near-nadir angles,¹⁰ making the inversion process unstable with noise. Moreover, other parameters are not constant, nor is their influence on the resulting wind estimate always understood.

In spite of all these complications, substantial progress has been made in the retrieval of high-resolution wind fields from SAR image data. One such example is illustrated here; several other (more or less successful) examples are given elsewhere in this issue.

STORMWATCH

ScanSAR imagery obtained under a Radarsat Applications Development and Research Opportunity (ADRO) project was acquired during the 1996–1997 northern winter off the U.S. East Coast (see the inside back cover). The ADRO products clearly illustrated the wealth of atmospheric expressions manifest in even

relatively narrow swath (300-km) ocean images. Many of these expressions had been seen in Seasat, but the wider swaths of Radarsat were able to capture much larger views of the synoptic patterns. For example, the cold air outbreak displayed on the easternmost swath on 14 January 1997 (inside back cover) shows a surprisingly coherent spatial evolution of the marine atmospheric boundary layer (MABL), beginning at the coast and extending well southeast past the Gulf Stream (see Sikora et al., this issue). Such a detailed evolution of the MABL at the surface would be impossible to observe with any other technique.

These early but limited observations of an often highly structured and evolving surface wind field were quite remarkable and spurred a plan for a more systematic collection program for the following winter. This more intense acquisition plan was devised by APL in cooperation with the U.S. National Oceanic and Atmospheric Administration’s National Environmental Satellite, Data, and Information Service (NOAA/NESDIS), which fortunately had data acquisition allotments from the Canadian Space Agency through a NASA agreement. The plan, spanning November 1997 through March 1998, specified sets of ascending wide ScanSAR passes at a 440-km width and ≈ 1500 -km length to be collected every third day off the U.S./Canadian East Coast (Fig. 1). The coverage pattern began in the east and continued westward, with adjacent (overlapping) swaths at 3-day intervals. The pattern repeated every 24 days. (Similar sets of descending passes also occurred, but those normally were not

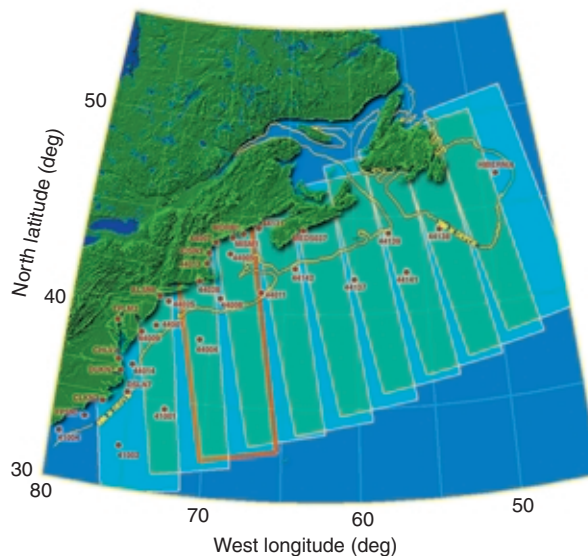


Figure 1. The region of interest for StormWatch coverage. A set of 10 Radarsat (440-km) passes is shown. Coverage accumulates from east to west at intervals of 3 days. Pass 10710, which occurred at 2230 GMT on 22 November 1997, is the subject of interest in this article and is bordered in orange. Also shown are the 200-m depth contours (yellow) and the positions of U.S. and Canadian buoys (red) useful for calibrating the SAR.

acquired.) This collection area contains many U.S. and Canadian buoys that are essential in the wind calibration strategy, as described by Thompson and Beal, this issue. Moreover, all the westernmost passes crossed over the Gulf Stream, which often creates an unstable boundary layer (warmer water provides buoyancy to the colder air). An unstable boundary layer can increase backscatter, giving the false impression of an increased surface wind speed.

Although originally conceived as an operational demonstration, the East Coast StormWatch coverage and data delivery for the winters of 1997–1998 and 1998–1999 did not approach the performance necessary for an operational product. There were many reasons for this shortfall: lack of priority in acquisition requests (i.e., conflicts with higher-priority users), months of delay in data transfer from the Canadian receiving station (Gatineau, Quebec) to the U.S. Alaska SAR Facility (ASF), similar delays at ASF in processing and delivery, and, as already mentioned, inadequate calibration in the wide swath modes. Nevertheless, progress has been substantial, as results in the following section will attest.

The 22 November Event in the Gulf of Maine

The first wide (440-km) ScanSAR pass in the StormWatch sequence for the 1997–1998 fall–winter series was acquired at 2230 GMT on 22 November (highlighted in Fig. 1). A high-resolution SAR-derived wind field from the northern end of the pass is shown on the outside cover of this issue. To better understand the features and to put the results in perspective, we examine here the meteorological events leading up to and occurring just after overpass time, as well as some of the other potentially relevant data around that time. We used model parameter fields produced by the U.S. Navy Fleet Numerical Meteorology and Oceanography Center in Monterey, California. This choice, although only one of several possible models, is especially convenient since it is routinely available twice a day. (Other options include models from the U.S. National Centers for Environmental Prediction, Suitland, Maryland; the British Meteorological Office, Bracknell, U.K.; and the European Center for Medium Range Weather Forecasting, Reading, U.K.)

The time sequence of pressure fields in Fig. 2 shows a deepening low-pressure system moving rapidly through the overpass region and toward the northeast. Ninety minutes after overpass time (2400 GMT) the low was moving south of Nova Scotia. Six hours later (0600 GMT, 23 November), it deepened further as it passed south of Newfoundland. A second set of six additional parameter fields, all 1.5 h after overpass time, is shown in Fig. 3. Model wind vectors (Fig. 3a) showed maximum winds around 20 m/s well to the east of the overpass, with counterclockwise circulation around the low pressure center producing northeasterly (from the northeast) winds at 15 m/s in the Gulf of Maine (northern portion of the overpass). Meanwhile, southeasterly winds in the south of the pass, working over a long fetch, produced waves as high as 5 m (Fig. 3b).

From the combination of wind and wave vectors, one can derive the “inverse wave age,” which is proportional to the local wind–wave slope. The inverse wave age is the ratio of the component of wind velocity traveling in the direction of the dominant waves to the dominant wave velocity. An inverse wave age of ≈ 1 implies equilibrium (wave growth rate = decay rate). Younger waves are steep and growing; older waves are smooth and decaying. For the same wind speed, young, steep, growing waves produce a higher radar return than old, smooth, decaying waves. Thus, wave age is another “contaminating” factor in the backscatter-to-wind

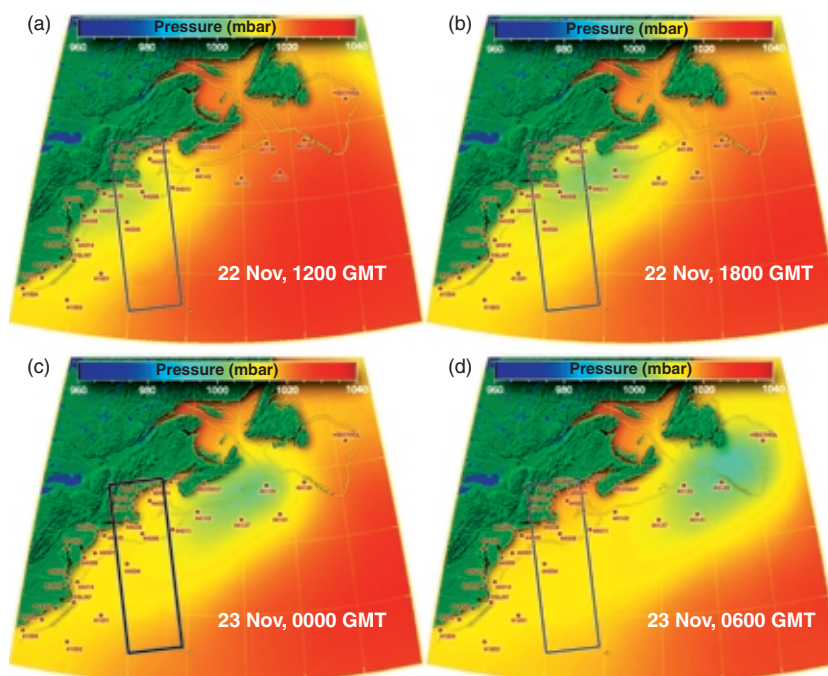


Figure 2. A set of four sequential model pressure fields around pass 10710 overpass time (2230 GMT), showing a deepening low pressure developing off Cape Hatteras and moving rapidly to the northeast. Overpass occurred 90 min before (c). Region shown is identical to that in Fig. 1.

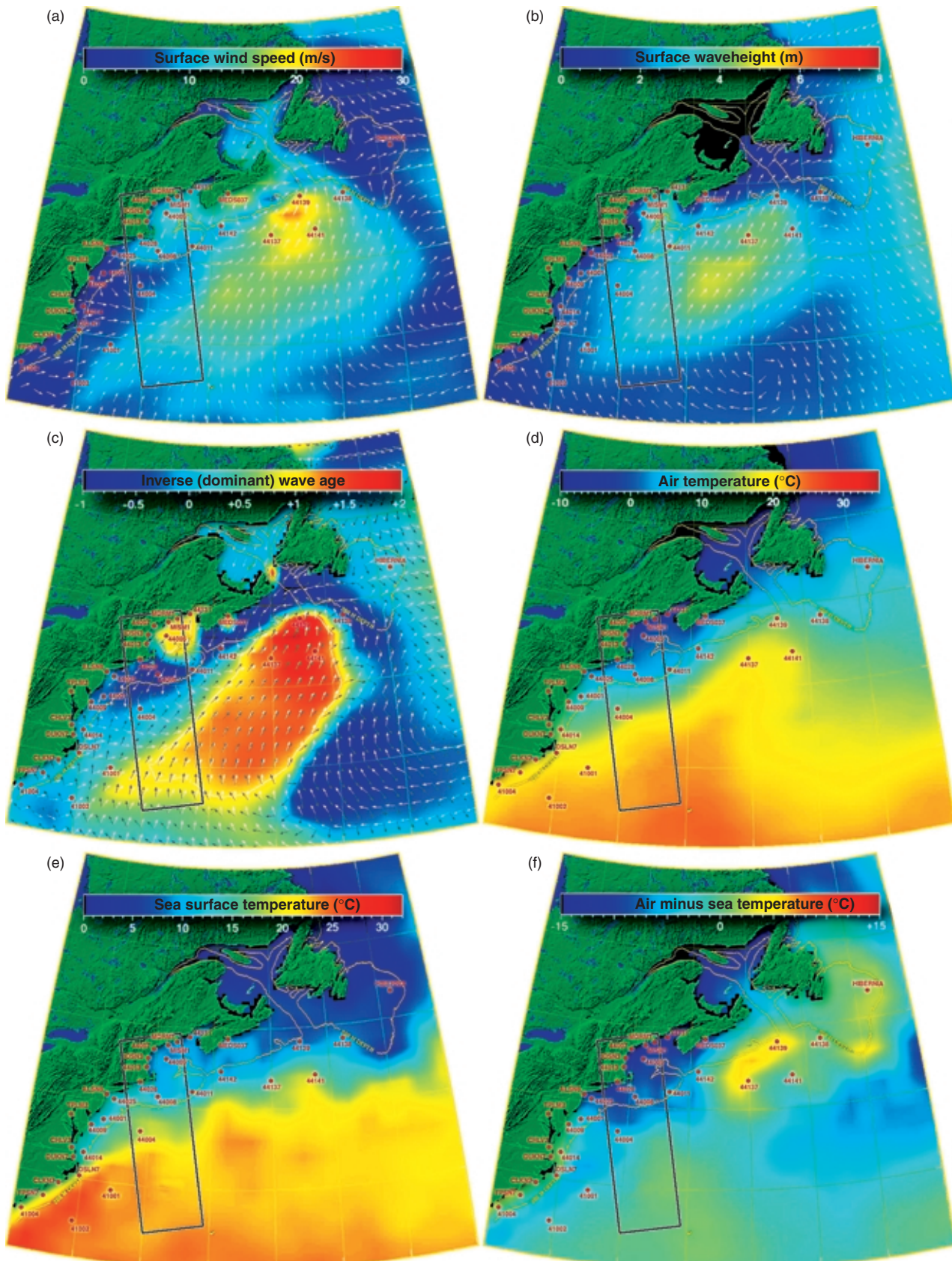


Figure 3. A set of six model parameter fields on 23 November at 0000 GMT illustrating (a) wind speed, (b) waveheight, (c) inverse wave age, (d) air temperature, (e) sea surface temperature, and (f) air-minus-sea temperature. Region shown is identical to that in Fig. 1.

relationship. Figure 3c shows the model inverse wave age field near overpass time. As expected, it was maximum where the wind was highest (where the waves were growing, but not necessarily the highest), but it also reached a secondary maximum in the Gulf of Maine near the northeastern corner of the SAR overpass. Here the wind opposed the waves, increased their slope (for the same wind speed), and so increased the backscatter, falsely indicating a higher than actual wind speed.

Figures 3d and 3e show model air and sea surface temperature, respectively, and Fig. 3f shows the difference between air and sea temperature (air minus sea), which is a measure of boundary-layer stability. Boundary-layer stability, as noted earlier, can also influence surface roughness, and therefore radar backscatter. An unstable boundary layer can lead to increased backscatter for the

same wind speed. The reverse condition is even more influential, however: an increasingly stable boundary layer (colder water below warmer air) can significantly suppress the surface roughness, indeed even quench the roughness for sufficiently high stability at low wind speeds. Figure 3f shows how the cold northeasterly winds produce an unstable boundary layer over the warmer Gulf of Maine. Although this instability does not significantly alter the mean backscatter, it does manifest itself in other ways in the SAR imagery. Roll vortices are the most obvious evidence of the instability. These vortices appear as patterns of order of kilometer scale, roughly aligned with the local wind vector (see, e.g., the articles by Brown and by Mourad et al., this issue).

Figures 4a–4d show four versions of Radarsat pass 10710 embedded in the model wind field (Fig. 3a)

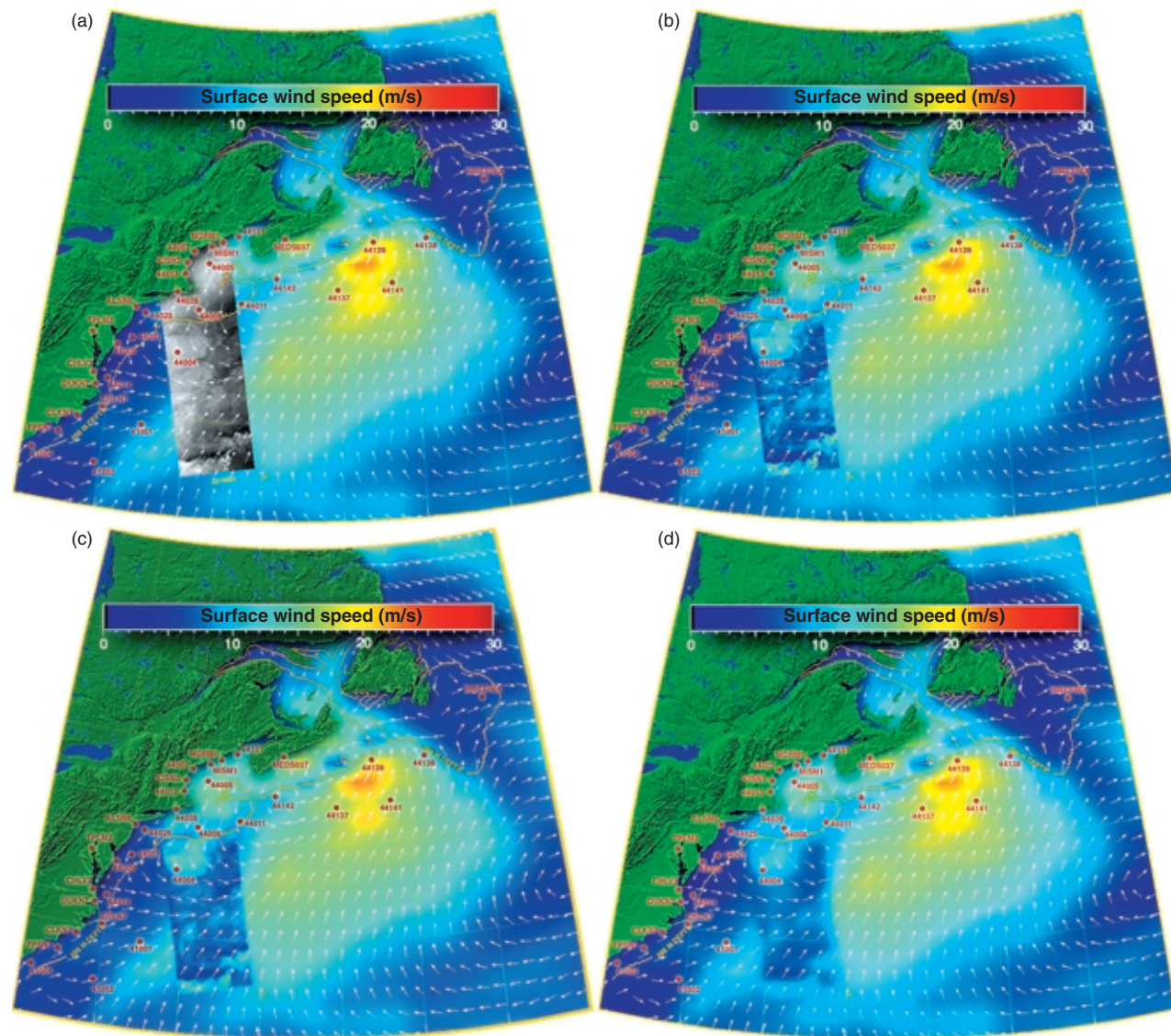


Figure 4. Radarsat pass 10710 embedded in the model wind field forecast at overpass time: (a) relative SAR backscatter and (b) high-, (c) medium-, and (d) low-resolution SAR wind speed. Region shown is identical to that in Fig. 1.

closest to the overpass time: (Fig. 4a) uncorrected (relative) radar backscatter, with the higher backscatter at the steeper radar incidence angles (satellite track is ascending to near-north, and the radar is right-looking); (4b) high-resolution (≈ 300 -m) SAR-derived wind speed (see Thompson and Beal, this issue); (4c) medium-resolution (smoothed to ≈ 3 km) SAR-derived wind field; and (4d) low-resolution (smoothed to ≈ 30 km) SAR-derived wind field. This low-resolution version approaches the resolution of the wind model (≈ 100 km) and is also quite similar to the resolution of conventional scatterometers. Without dwelling on the finer details for the moment, it is clear that the SAR wind estimates were lower than those of the model throughout the southern two-thirds of the pass. Unfortunately, there is no way to determine in this case which was more correct, the model or the SAR. All the working buoys are located in the northern third of the pass. The model may have overestimated the magnitude of the wind in the wake of the storm. On the other hand, the SAR estimates in the northern third of the pass agree nicely with the model, at least on the large scale. In this region, model, buoy, and SAR patterns of wind direction all agreed remarkably well, so we are confident that the finer features of the SAR wind field are also real and accurately depicted.

On the fine scale, SAR reveals spatial structure over a vast region of the wind field not even suggested by the model, and certainly not measurable over such scales by any other coarse grid technique. The enhanced SAR image in Fig. 5a (as well as the cover of this issue) shows the remarkable detail in the wind field structure all along the New England coast. The wind scale is expanded and the wind field is differentiated in the mean crosswind direction to further emphasize the subtleties. For this figure, a topological landform map¹¹ has replaced the land portion of the

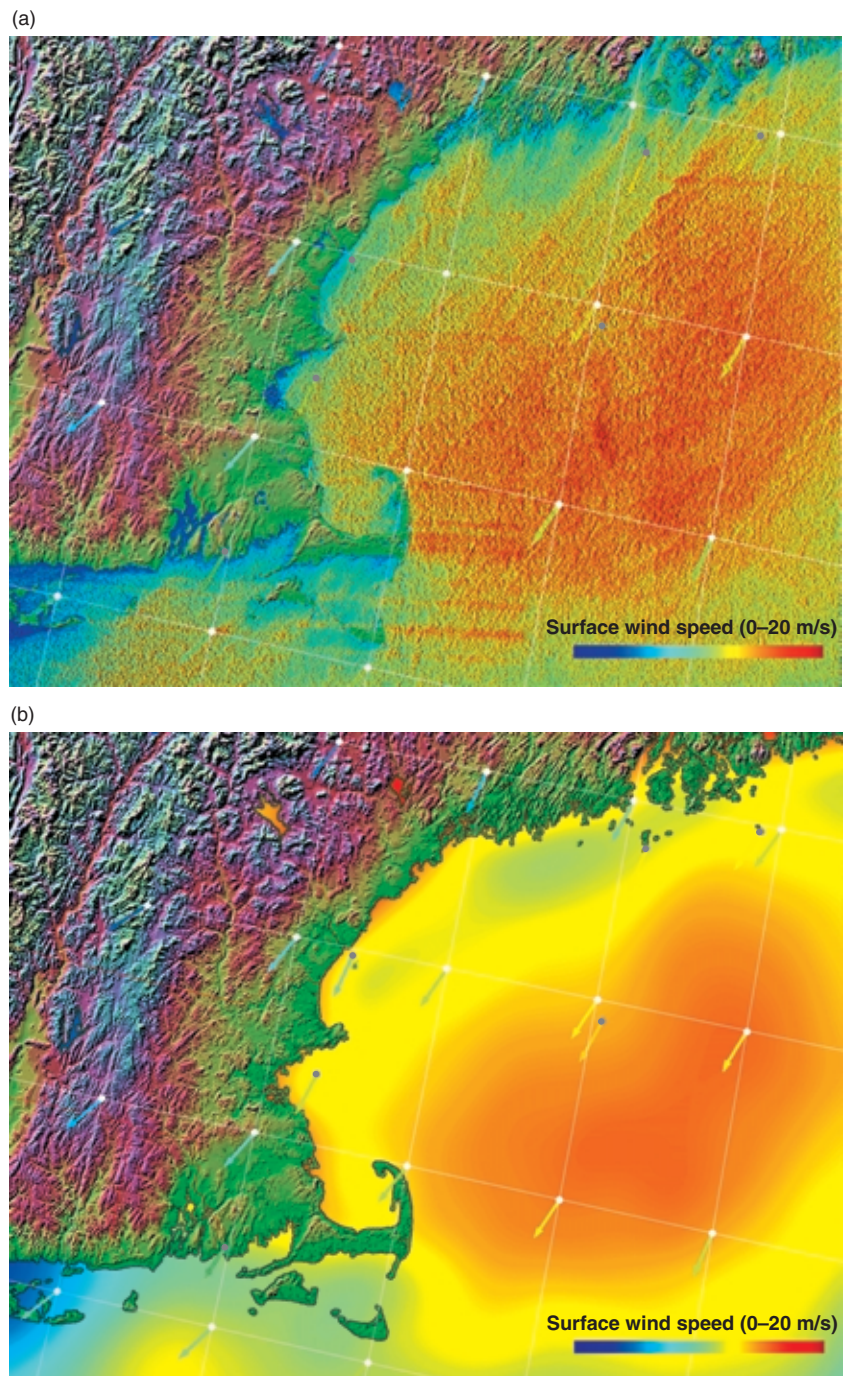


Figure 5. (a) SAR wind field in the Gulf of Maine at a spatial resolution of 300 m (Radarsat pass 10710, 22 November 1997). Horizontal dimension is 440 km. Also shown are model wind vectors (white dots) and buoy wind vectors (gray dots). Land portion has been replaced with topography.¹¹ (b) Same as Fig. 5a, but spatially smoothed to 25 km to simulate the resolution of a conventional scatterometer. Spatial structure is absent, and strong radar return from the (underlying) land backscatter produces the false impression of high winds along the coast.

radar image. The topology is useful for judging how the upwind land features might influence the wind field morphology. Note the extremely high variability of the wind field near the shore and its general sheltering effect. Clearly, the large-scale mean is a poor indicator

of the wind speed at any given point along the coast. Often the stronger wind features appear to be associated with longer fetches available from the inland bays and estuaries. Obvious signs of atmospheric instability are also evident in the overall streakiness roughly aligned with the wind field direction. These instabilities appear to produce large crosswind gradients in wind magnitude. Independent validation of many of these phenomena is difficult if not impossible, simply because no other sensor has both the resolution and perspective of the SAR. The best that can be done is to compare relevant spatial averages from the SAR with corresponding resolutions from other sensors, or, through a Taylor-like hypothesis, to associate elongated areas of the SAR wind map with time-averaged buoy estimates.

To further emphasize the unique spatial resolution of the SAR, especially its superiority in coastal areas, Fig. 5b shows a smoothed version of Fig. 5a that simulates a conventional scatterometer product with a typical spatial resolution of 25 km. The spatial structure has disappeared, of course, but more significantly the coastal regions and lakes now show much higher winds than actually existed. Contamination arising in a scatterometer from the adjoining land, for off-nadir angles higher than about 30°, completely overwhelms the lower backscatter of the nearby water. This is a major limitation of conventional wind scatterometry, rendering its results unreliable within about 50 to 100 km of the coast. It is also a reminder of another limitation of both scatterometers and numerical models, even in noncoastal regions: the actual wind field at a particular point is often poorly represented by an average over many tens of kilometers. This limitation is especially acute around coasts, fronts, cold air outbreaks, and polar and tropical storms, where the spatial (and, by implication, the temporal) fluctuations of the true wind field may often exceed the mean.

Problems and Prospects

There is no question that wide swath SAR can, under favorable conditions, deliver a unique and valuable perspective of the true wind field that would otherwise remain obscured in the best numerical model and conventional sensor estimates. However, this uniquely superior aspect of SAR must be weighed against several limitations, especially if the goal is a routine, global, near-real-time operational wind product. These limitations can be categorized as scientific, technical (or engineering), and organizational (or political).

Scientifically, as mentioned earlier, the physics of radar ocean scattering is far from simple on the large scale sampled by conventional scatterometers and radiometers. Scattering physics is even more complicated

on the small scales representative of SAR imagery. Many potentially relevant variables exist, including the

- Wind vector and its three-dimensional spectrum
- Wave vector and its two-dimensional spectrum
- Wind vector height profile as a function of boundary-layer stability
- Water surface tension and dielectric constant as a function of impurity concentration
- Extent of wave breaking as a function of both wind and waves
- Radar frequency and polarization
- Nonlinear interaction of all of these with one another on spatial scales of only a few hundred meters

Many of the interactions are significant but only partially understood, and field experiments to probe their relationships are often difficult and expensive or impractical.

The problem seems intractable, yet some progress is possible. The motivation is strong. Wind estimates from SAR, if they can be produced on spatial scales of only a few hundred meters, even if only approximately correct, will greatly exceed the capabilities of any other technique.

The most acute and intolerable error source in SAR wind estimates comes from the uncertainty in *a priori* estimates of local wind direction with which to enter the backscatter-to-wind conversion equation. This problem is discussed extensively by many authors in this issue (e.g., Vachon et al.; Gower and Skey; Thompson and Beal; Horstmann et al.). No satisfactory solution for the problem has yet been proposed that will work under all circumstances. The problem is most severe in rapidly changing winds, fronts, and storms. Needed is some kind of optimum blending of information within the SAR image itself with model forecasts and coarser-resolution sensors. Although some progress has been made on this front, much more is still required.

From an engineering (technical) perspective, probably the largest obstacle to a reliable operational wind product is inadequate system calibration. System stability is required both in the long- and short-term. Although elegant in concept, the ScanSAR multibeam technique severely constrains, in particular, spacecraft attitude control for radiometrically calibrated products. As Fig. 6 illustrates, a seamless correction for the multibeam antenna pattern is especially limited by spacecraft attitude uncertainty at the beam crossover points, where the antenna gain derivative with respect to off-nadir angle is highest. The effect is exacerbated at high winds by the decreasing slope of the radar backscatter-to-wind relationship. For example, a typical gain slope at the ScanSAR antenna beam crossover points is ≈ 3 dB per degree of elevation angle change; a typical backscatter-to-wind-speed change (at 22°

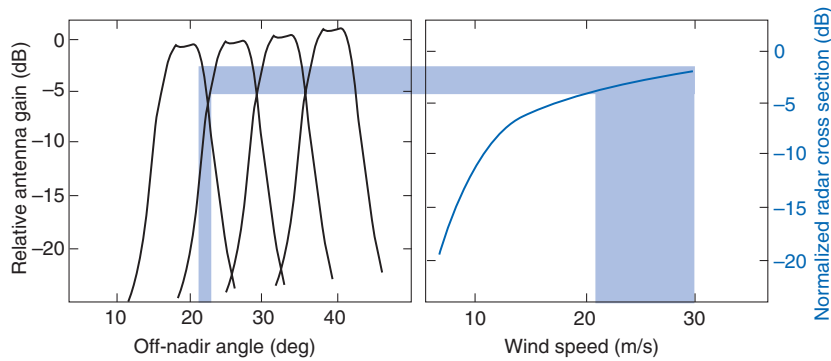


Figure 6. Backscatter-to-wind SAR inversion is sensitive to uncertainties (blue highlight) in spacecraft roll angle at the crossover points of the ScanSAR multiple antenna beams. A small uncertainty in roll (off-nadir) angle (left) can produce an uncertainty in antenna gain that translates into a large uncertainty in wind speed (right).

elevation, and around 25 m/s wind speed) is ≈ 0.05 dB per m/s. Thus a spacecraft roll uncertainty of only $\approx 0.1^\circ$ can lead to a wind speed error of ≈ 6 m/s at 25 m/s, or $\approx 25\%$. The Radarsat antenna pointing accuracy specification⁷ is 0.2° ; the attitude control specification is $\approx 0.05^\circ$.

This performance is already on the verge of being inadequate for the wind application, but unfortunately it is only one of several sources of calibration error. Another is gain uncertainty in the end-to-end system transfer function, typified by a time-dependent transmitted power or a time-dependent receiver gain (e.g., automatic gain control, or analog-to-digital converter saturation); yet another is the uncertainty in the primary calibration standard itself. For example, the Amazon Rain Forest in Brazil is often used as a primary reflectivity standard, but it is not homogeneous, nor is it invariant with time. Clearly, a long-term, closed-loop calibration strategy must be an integral part of any future operational global wind monitoring system employing a ScanSAR technique.

Organizationally (or politically), there also is much to be accomplished before routine global operational wind products from SAR can be realized. For twice-daily coverage of the Earth poleward of 45° latitude (a minimum requirement, according to potential users in both the U.S. Coast Guard and the National Weather Service), at least four wide swath orbiting ScanSARs of the Radarsat variety (or two-satellite double-sided coverage) are needed. This becomes clear by noting that the Earth rotates ≈ 2800 km at the equator (or ≈ 2000 km at 45° latitude) during a typical Radarsat orbit of 100 min. Thus a configuration of four 500-km ScanSARs in identical polar orbits, each separated from its nearest neighbor by a quarter orbit (25 min), could create a 2000-km swath over most points on the Earth twice a day (using both ascending and descending passes). For a Sun-synchronous orbit (preferable to

maximize solar power), the entire 2000-km swath could be constructed within a 75-min (± 37.5 -min) interval over any given region. At any given point, acquisitions would occur at the same local time.

Of course, this is only one possible coverage scenario; Holt and Hilland (this issue) consider others in more detail. The main point to be made here is that one or even two (single-sided) ScanSARs, although valuable for algorithm development and applications demonstrations, will not constitute an operational configuration. For operational viability we need organizational (funding agency) commitment.

This commitment must be built and justified upon clearly articulated user needs originating from the various multinational weather services and coast guards. The process, however, is highly iterative. The users cannot articulate a need unless they know what is possible and practical from a scientific and engineering perspective. So the science and technology must drive, as well as be driven by, the users.

Well-designed and executed operational demonstrations can be conducted with the coming suite of ScanSARs, and special attention can be given to user needs and feedback. One such demonstration in the Gulf of Alaska is already well under way and expected to continue through two winters (see Pichel and Clemente-Colón, this issue; also Monaldo, this issue). Other such demonstrations are being planned for the Envisat era starting in 2001 (see Attema et al., and also Johannessen, this issue).

As Fig. 7 shows, the sum of all available ScanSAR swaths expected in the next 3 years from the European Envisat, the Canadian Radarsat, and the Japanese

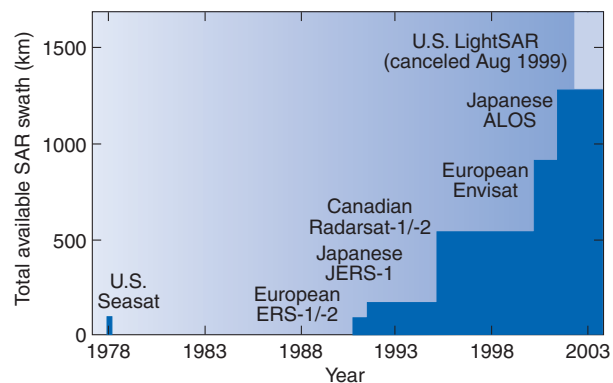


Figure 7. Timeline of civilian spaceborne SARs from 1978 to 2003, shown as an accumulating composite swath width. (Chart is accurate only to within 100 km or so.)

Advanced Land Observing System (ALOS) will probably exceed 1200 km. With the addition of the U.S. LightSAR (recently canceled), it might have exceeded 1500 km. Coordination of these multinational platforms, accompanied by an enlightened data distribution policy, could go far toward providing an operational and affordable global SAR wind product.

One possible initial coverage scenario is shown in Fig. 8, derived as a natural extension of the recently completed StormWatch along the North American coast and the Gulf of Alaska Demonstration currently under way. The figure highlights four regions in the Northern Hemisphere that routinely experience dangerous winter storms, with an associated high toll on life and property. Such an international demonstration would of course require subscription and commitment from the major SAR-capable nations. From the purely humanitarian perspective, however, international cooperation on this scale would seem to be an imperative at this formative stage in the development and application of SAR.

CONCLUSION

In the last 20 years, there has been a gradually accelerating maturation of both the science and technology of SAR for marine applications. With the well-calibrated imagery from the European ERS-1 and -2 and the successful demonstration of the wide swath ScanSAR in the Canadian Radarsat, strong evidence



Figure 8. Potential regions of focus for cross-calibrating a global SAR wind monitoring system.

is emerging that a synchronized suite of well-calibrated and stable ScanSARs could deliver high-resolution operational wind fields. Progress is still needed in several areas of science and technology. Perhaps the most challenging technical problem is the execution of a viable end-to-end calibration strategy that will allow a robust and reliable inversion of the backscatter-to-wind relationship. There is every reason to believe that this obstacle will be overcome soon, either in the later years of Radarsat-1 or the early years of Envisat. Even more challenging, however, will be a demonstration sufficient to convince operational users that a ScanSAR wind product can be accurate, timely, and affordable.

REFERENCES

- ¹Wiley, C. A., "Synthetic Aperture Radars—A Paradigm for Technology Evolution," *IEEE Trans. Aerosp. Electron. Syst.* **AES-21**, 440-443 (1985).
- ²Cutrona, L. J., and Hall, G. O., "A Comparison of Techniques for Achieving Fine Azimuth Resolution," *IRE Trans. Mil. Electron.* **MIL-6**, 119-133 (1962).
- ³Raney, R. K., "Radar Fundamentals: Technical Perspective," in *Principles and Applications of Imaging Radar, Manual of Remote Sensing*, Vol. 2, Wiley, New York, pp. 9-130 (1998).
- ⁴Jordan, R. L., "The Seasat-A Synthetic Aperture Radar System," *IEEE J. Oceanic Eng.* **OE-5**(2), 154-164 (Apr 1980).
- ⁵*Seeing Earth in a New Way: SIR-C/X SAR*, Report 400-823, Jet Propulsion Laboratory, Pasadena, CA (May 1999).
- ⁶Attema, E., "The Active Microwave Instrument On-board the ERS-1 Satellite," *Proc. IEEE* **79**(6), 791-799 (Jun 1991).
- ⁷Raney, R. K., Luscombe, A. P., Langham, E. J., and Ahmed, S., "Radarsat," *Proc. IEEE* **79**(6), 839-849 (Jun 1991).
- ⁸Tomiyasu, K., "Conceptual Performance of a Satellite-borne Wide Swath Synthetic Aperture Radar," *IEEE Trans. Geosci. Remote Sens.* **GE-19**(2), 108-116 (Apr 1981).
- ⁹Moore, R. K., Claassen, J. P., and Lin, Y. H., "Scanning Spaceborne Synthetic Aperture Radar with an Integrated Radiometer," *IEEE Trans. Aerosp. Electron. Syst.* **AES-17**(3), 410-421 (May 1981).
- ¹⁰Donnelly, W. J., Carswell, J. R., McIntosh, R. E., Chang, P. S., Wilkerson, J., et al., "Revised Ocean Backscatter Models at C and Ku Band Under High Wind Conditions," *J. Geophys. Res.* **104**(C5), 11,485-11,498 (May 1999).
- ¹¹Stern, R. E., *Color Landform Atlas of the United States*, available at <http://fermi.jhuapl.edu/states> (accessed 9 Nov 1999).

ACKNOWLEDGMENT: This work was supported through Office of Naval Research Grant N00014-96-1-0376, NOAA Cooperative Agreement NA77ECO554, and discretionary funds from the JHU/APL Director's Office. I am grateful to my APL colleagues Frank Monaldo, Donald Thompson, and Keith Raney for their valuable ideas and comments.

THE AUTHOR

ROBERT C. BEAL is with The Johns Hopkins University Applied Physics Laboratory, Laurel, MD. His e-mail address is robert.beal@jhuapl.edu.